Ekoloji 27(106): 579-589 (2018)

Study on Mechanism of Air-Floating Separation for Residual Film and Seed Cotton

Gaili Gao [1*], Yinhui Feng [1#], Yongxian He [1]

[1] College of Engineering, China Agricultural University, CHINA

[*] Corresponding author: ggl1965@126.com; [#] Co-first author

Abstract

Xinjiang is the main planting area of cotton in China. The frost-free period in this area is short and the annual rainfall is less-than 200 mm. Wide-film cotton planting technology is widely used. The filming rate of cotton field is almost 100%, about 60000 to 80000 tons of broken residual films are newly produced every year, and has caused serious pollution in farmland. Mechanized harvesting has a large amount of residual films in seed cotton, which affects not only the quality of seed cotton, but that of ginned cotton. In this paper, aiming at the key technical problem of removing cotton contaminant, i.e., residual film, a novel model is created. It is the first time to propose that the seed cotton is tore into a movable 'wave-pattern' thin layer by blowing air so that the residual film is fully exposed and then cleared by a suction-cleaner. To acquire such a seed cotton layer, upward airflows that flow in the 'wave-pattern' are added to a separation chamber transversely in the model, and airflows that can carry the seed cotton forward are added to the chamber longitudinally. First, the airflow distribution characteristics in the separation chamber are analyzed within a 2D model. The experiment shows that the airflow field is divided into three areas, the bottom area is diffusion zone of the airflow from airflow-holes on a hole-plate, where the airflow velocity is high, unstable and attenuate quickly, and the airflow field is mainly influenced by the airflow velocities at airflow-holes and its dip angle; the airflow field in the middle area is more stable and the airflow velocity is obviously lower than that in the bottom area, and the airflow direction is mainly affected by the dip angles of walls of cotton-inlet and cotton-outlet; and the airflow in the upper area has relatively high velocity due to the suction-cleaner. Therefore, the seed cotton should run in the middle area of airflow field. By further analyzing the orthogonal experiment results, the optimized values of three key geometric parameters are gained, that is, the height of separation chamber is 1.40m, the dip angle of walls of cotton-inlet and cotton-outlet is 80.00°, and that of airflow-holes on the hole-plate is 8.00°. Second, the airflow field characteristics are analyzed in the 3D flow field to acquire the velocities of 'wave-pattern' airflow. The results show that in order for the airflow velocity to stay in the range of 1.20-3.00m/s in the middle area of airflow field, the range of airflow velocity at the inlet of each row of airflow-hole on the hole-plate should be 8.00-14.00 m/s.

Keywords: air-floating separation, seed cotton, residual film, remove

Gao G, Feng Y, He Y (2018) Study on Mechanism of Air-Floating Separation for Residual Film and Seed Cotton. Ekoloji 27(106): 579-589.

INTRODUCTION

Xinjiang is the main planting area of cotton in China. The frost-free period in this area is short and the annual rainfall is less-than 200 mm. Wide-film cotton planting technology is widely used. The filming rate of cotton field is almost 100%, and about 60000 to 80000 tons of broken residual films are newly produced every year. The polyethylene plastic residual film is stable and difficult to degrade. Long-time and large-scale plastic film mulching has caused serious pollution in farmland (Wang et al. 2016). Mechanized harvesting has a large amount of residual films in seed cotton, which affects not only the quality of seed cotton, but that of ginned cotton. The residual film is classified as a kind of cotton foreign fibers, but its color is very close to cotton and it is very easily broken by the hit of mechanical components on the production line, so it is almost the most difficult to identify and remove it. In recent years, in order to identify the residual film, the domestic and foreign researchers focused their attention on choosing different kinds of the sources of illumination and using various kinds of novel image processing algorithms (Zhang and Li 2014, Guo et al. 2014).

For the used sources of illumination, a laser imaging method is suggested to distinguish most of the white foreign fibers from cotton based on the difference of microstructure of sample surface. The method using a double-light illumination of light emitting diode (LED) and laser for imaging was also presented. It was indicated that the successful detecting rates of white foreign fibers and other colored fibers using the fixed threshold binary algorithm could reach up to 84.1% and

 Received: 10 Jul 2017 / Accepted: 16 Sep 2018

93.9%, respectively (Liu et al. 2014 Wang et al. 2015a, Zhang et al. 2016). For detecting the foreign fibers in seed cotton, an experiment was done by using the double-light illumination. The detecting rates of white and color foreign fibers were up to 74.7% and 70.8%, respectively (Wei et al. 2017). The blue and UV LEDs are also selected as the excitation sources. The blue LED light provided optimal excitation light for bark, brown leaf, bract, green leaf, hull, and stem, while the UV LED light provided optimal excitation light for paper, plastic bag, plastic packaging, seed, seed coat, and twine (Mustafic et al. 2014, 2015). Furthermore, the methods of chromatic polarization imaging, or polarization channel added to the UV channel were adopted for the online detection of colorless plastic contaminants (Peng et al. 2015, Zhang et al. 2017a). In a recent review paper, it was mentioned that the near infrared spectroscopy (NIRS) was an emerging, non-invasive, multi-index, simple preparation of sample process analytical technique suitable for cotton quality assessment (Zhou et al. 2016). For example, a short wave near infrared hyperspectral imaging (HSI) system using the transmittance mode was used to detect common types of foreign matter hidden within the cotton lint. This study indicated that it was feasible to detect botanical (e.g. seed coat, seed meat, stem, and leaf) and non-botanical (e.g. paper, and plastic package) types of foreign matter (Zhang et al. 2017b). The optimal wavelengths from the visible to near infrared spectra of the hyperspectral imaging data, and a Fourier transform infrared (FTIR) microscope equipped with a focal plane array detector (FPA) were chosen for cotton foreign matter classification and identification, respectively (Jiang and Li 2015b, Cintron and Rodgers 2017). And other hyperspectral and multispectral imaging systems were describes to discriminate major types of foreign matters in cotton lint. The results showed that the mean spectra of all the 15 types of cotton foreign matters were different from that of the lint (Jiang and Li 2015a, Li et al. 2015). In addition, the pulsed thermographic analysis is explored to detect and identify cotton foreign matter (Kuzy and Li 2017). The above is based on the light propagation, absorption and reflection characteristics of different substances under different illumination.

For the image processing algorithm, an improved ant colony optimization for feature selection was proposed. The algorithm was tested in the datasets of foreign fibers in cotton and comparisons with other methods were made. The experimental results showed that the algorithm could find the high-quality subsets with smaller size and high classification accuracy (Zhao et al. 2014). Three metaheuristic-based feature selection approaches for cotton foreign fibers recognition, which are particle swarm optimization, ant colony optimization and genetic algorithm, were also described. The results showed that they could efficiently find the optimal feature sets consisting of a few features (Zhao et al. 2016b). And the efficient classifier based on the kernel extreme learning machine (KELM) showed that the system could achieve classification accuracy as high as 93.57% (Zhao et al. 2016a). The foreign fiber clustering analysis algorithm during the processing of cotton textile was investigated, and the lowest recognition rate is 85% (Du et al. 2017). The regression equation was compiled to produce the foreign fiber yarn faults model. The actual defects from the experiment were compared with the predicted theoretical defects from the equation, and the prediction accuracy was found to reach more than 95% (Du et al. 2016). And the classification processing method of cotton foreign fibers based on probability statistics and BP neural network was also used (Wang et al. 2014). In addition, the fast image segmentation algorithm based on image blocking and local Otsu's method was for detecting the pseudo-foreign fiber, and the performance of RBF kernel SVM was the best among the three classifiers with average recognition rate of 95.60% (Wang et al. 2015b, 2015c).

The above-mentioned technologies were used in the apparatus for removing foreign fibers in pneumatically conveyed cotton, and the foreign fibers are detected by the CCD cameras and removed by the high-pressure air from the nozzles. However, there are two major defects for the apparatus: (1) In the pneumatic conveying pipeline, the movement of cotton and foreign fibers are turbulent and irregular. At the upstream location of the CCD cameras, the foreign fibers are seen and located, but the foreign fibers cannot be found accurately at the downstream location of nozzles. That is to say, the positions of foreign fibers are 'turbulent'. (2) In the lint production line, the amount of cotton flowing in the pipeline with1m of width is about 4000 kg/h, and the speed of cotton in the pipeline is at least 12 m/s. Under such conditions, it is no longer suitable to detect the foreign fibers by the CCD cameras, that is, the CCD cameras have no ability to detect all the foreign fibers in cotton. In view of this, in the paper, aiming at the key technical problem of removing cotton contaminant, i.e., residual film, a novel model is created. It is the first time to propose that the seed cotton is tore into a movable 'wave-pattern' thin layer by blowing air so that the residual film is fully exposed and then cleared by a

suction-cleaner. The software ANSYS R15.0 is used to simulate the airflow field characteristics of separation chamber in the model, and an orthogonal experiment method is used to analyze the results.

MODEL OF AIR-FLOATING SEPARATION

Mechanism of Air-Floating Separation for Residual Film and Seed Cotton

The air-floating velocity of the single seed cotton is about 3.0-5.0 m/s, and that of the residual film is about 0.3-1.2 m/s (Guo et al. 2011). That is, when the upward airflow velocity is greater than 1.20 m/s, the residual film rises, and when it is greater than 3.00m/s, some of the seed cottons also move upwards. The seed cottons are in masses, while the residual films are flaky. The air-floating velocity of residual film in a closed cavity is far less than that of seed cotton. Therefore, air-floating separation for the residual film and seed cotton can be realized by the difference of air-floating velocity between the two. To expose the residual film fully to the surface layer of seed cotton, the seed cotton layer in the closed cavity should be as thin as possible. To guarantee sufficient cotton throughput, the seed cotton layer is designed in the 'wave-pattern' so that the seed cotton can be tore into thin layers within limited width. To acquire the 'wave-pattern' seed cotton layer, upward airflows that flow in the 'wave-pattern' are added to the closed cavity transversely, at the parts where the airflow velocity is high, the seed cotton moves upward rapidly, and at the parts where the velocity is low, it moves upward slowly; and the airflows that can carry seed cotton forward should be provided longitudinally in the closed cavity, which help form the movable 'wave-pattern' seed cotton layer. The thickness of the seed cotton layer is set by adjusting the difference between the airflow velocity at the wave crest of the 'wave-pattern' and the wave trough of it.

Model of Air-Floating Separation for Residual Film and Seed Cotton

A novel model of air-floating separation for the residual film and seed cotton is created in accordance with the separation mechanism above, as shown in **Fig. 1**. It mainly consists of a separation chamber, an airflow component under it, a suction-cleaner above it, a cotton-inlet to its left and a cotton-outlet to its right. When it works, the seed cotton containing the residual film enters the separation chamber through the cotton-inlet. Airflow-holes of the airflow component give out airflows that flow upwards, though a little tilted. The component force of airflows is, vertically, equal to the gravity of seed cotton in magnitude, but opposite in direction. It can keep the seed cotton in suspension. However the gravity of residual film is smaller than the component force of airflows, the residual film moves upwards, and it is absorbed and cleared when getting close to the suction-cleaner. Horizontally, the seed cotton moves towards the cotton-outlet duo to the horizontal component force of airflows and is discharged from the cotton-outlet, thereby separating the residual film from the seed cotton.

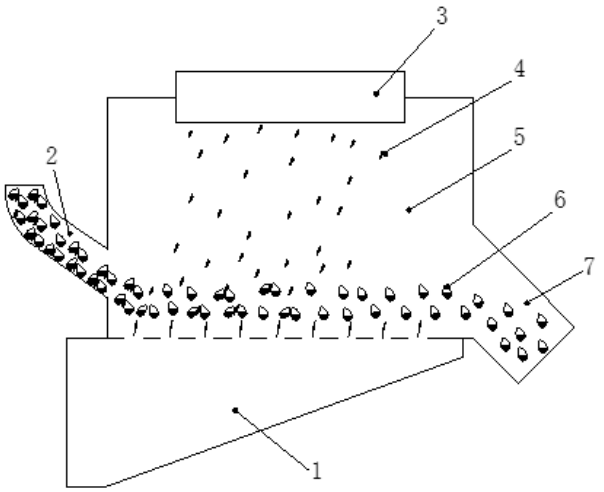

1. Airflow component 2. Cotton-inlet 3. Suction-cleaner 4. Residual film 5. Separation chamber 6. Seed cotton 7. Cotton-outlet

Fig. 1. Model of Air-floating Separation

In **Fig. 1**, the airflow is forced into the separation chamber from the airflow-holes of airflow component. The airflow velocity decreases quickly in separation chamber. When the velocity reduces to the same as the air-floating velocity of seed cotton, the seed cotton doesn't go up. If the airflow velocity is different at different positions in the transverse direction of separation chamber, the seed cotton has different air-floating height. When the airflow velocity is low, the air-floating height of seed cotton is also low, and the force of airflow on the seed cotton is small. Conversely, the air-floating height is high, and the force of airflow is huge. The airflow velocity should be supplied in the pattern of either 'high-low-high-low' or 'high-medium-low-medium-high-medium-low' so that the air-floating height of seed cotton is changed regularly in tandem with the velocity variation, like a wave, that is, 'wave-pattern' (**Fig. 2**). In this way, the seed cotton layer can be effectively thinned.

To achieve well-distributed adsorption of residual film, two negative-pressure reticulated cylinders with the same structure and shape are required as the suction-cleaner. In the model of air-floating separation, the front left lower corner is used as the coordinate

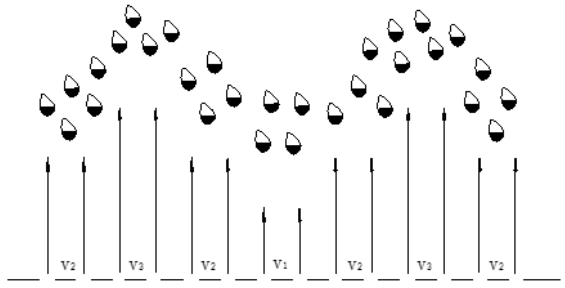

Fig. 2. Airflow Velocity of 'Wave-pattern'

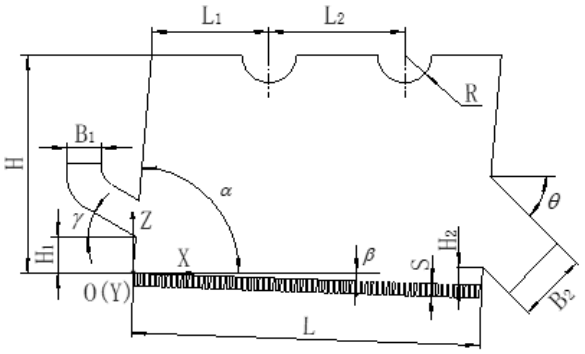

(a) Geometric parameters in front view

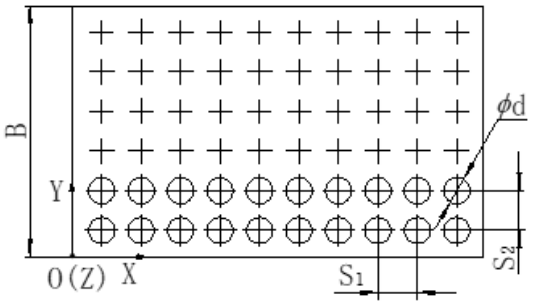

(b) Geometric parameters related to hole-plate in vertical view

Fig. 3. Geometric Parameters for Model of Air-floating Separation

origin O; the OX axis is located in the front of model and is horizontally to the right (i.e. the longitudinal direction of separation chamber); the OY axis is at the same horizontal plane as the OX axis, and the positive direction points to the rear of model (i.e. the transverse direction of it); the OZ axis is perpendicular to the XOY plane, and its positive direction is upward; and the Cartesian coordinate OXYZ is established, as shown in **Fig. 3**. The main geometric parameters of model are the lengthL, width B and height H of separation chamber; the diameter ∅ d, dip angle β, longitudinal spacing S_1 and lateral spacing S_2 of airflow-holes on the hole-plate of airflow component; the thickness Sof hole-plate; the width B_1, dipangle γ and height position H_1 of the cotton-inlet; the width B_2, dip angle θ and height position H_2 of the cotton-outlet; the dip angle $\alpha$of walls of cotton-inlet and cotton-outlet; the radius R of reticulated cylinders and their horizontal positions L_1 and L_2 Its kinematic parameters are the airflow velocity Vat the inlet of airflow-hole and velocity V_1 of seed cotton at the cotton-inlet.

COMPUTATIONAL FLUID DYNAMICS MODEL

Governing Equations

The mass and momentum conservation equations may be written as (Yuan et al. 2013):

$$\frac{\partial \rho}{\partial t} + \frac{\partial}{\partial x_i}(\rho u_i) = 0 \quad (1)$$

$$\frac{\partial}{\partial t}(\rho u_i) + \frac{\partial}{\partial x_j}(\rho u_i u_j) = -\frac{\partial p}{\partial x_i} + \frac{\partial}{\partial x_j}\left(\mu \frac{\partial u_i}{\partial x_j} - \rho \overline{u_i' u_j'}\right) + S_i \quad (2)$$

where ρ is the air density (kg/m^3), μ is the air dynamic viscosity(Pa. s), p is the pressure (Pa), u_i andu_j are respectively correspondent with the velocity component in the x_i and x_j directions (m/s), u_i' and u_j' are respectively correspondent with the fluctuating velocity in the x_i and x_j directions (m/s), $\overline{u_i' u_j'}$ is average value of u_i' multiplied by u_i', S_i is the source term in the x_i direction.

The standard k-ε model is used which applies to the strong swirl and curved wall flow. The turbulent kinetic energy and turbulent dissipation rate equations are defined as (Yuan et al. 2013):

$$\frac{\partial}{\partial t}(\rho k) + \frac{\partial}{\partial x_i}(\rho k u_i) = \frac{\partial}{\partial x_j}\left[\left(\mu + \frac{\mu_t}{\sigma_k}\right)\frac{\partial k}{\partial x_j}\right] + G_k + G_b - \rho\varepsilon - Y_M + S_k \quad (3)$$

$$\frac{\partial}{\partial t}(\rho \varepsilon) + \frac{\partial}{\partial x_i}(\rho \varepsilon u_i) = \frac{\partial}{\partial x_j}\left[\left(\mu + \frac{\mu_t}{\sigma_\varepsilon}\right)\frac{\partial \varepsilon}{\partial x_j}\right] + C_{1\varepsilon}\frac{\varepsilon}{k}(G_k + C_{3\varepsilon}G_b) - C_{2\varepsilon}\rho\frac{\varepsilon^2}{k} + S_\varepsilon \quad (4)$$

where k is the turbulent kinetic energy (J), ε is the turbulent dissipation rate, μ_t is the turbulence viscosity (Pa. s), σ_k and σ_ε are respectively the Prandtl numbers of turbulent kinetic energy and turbulent dissipation rate, G_k and G_b are the turbulent kinetic energy generation terms caused by average velocity gradient and buoyancy, respectively, Y_M is influence of fluctuating expansion of compressible turbulent flow on total dissipation rate, S_k and S_ε are the user-defining items. By experience we have $C_{1\varepsilon} = 1.44$, $C_{2\varepsilon} = 1.92$, $C_{3\varepsilon} = 0.09$.

In this paper, the drag force, gravity and buoyancy of seed cotton and residual film are taken into account. The seed cotton and residual film are used as discrete terms, and the Discrete Phase Model (DPM) is suggested. The kinematic equation of particle in the x_i direction is as follows:

$$\frac{du_{pi}}{dt} = \frac{18\mu}{\rho_p d_p^2}\frac{C_D R_e}{24}(u_i - u_{pi}) + \frac{\rho_p - \rho}{\rho_p} g_i \quad (5)$$

where u_{pi} is the velocity of particle in the $x_i$direction (m/s), ρ_p is the density of particle (kg/m^3), d_p is the diameter of particle (m), g_i is the gravity acceleration in the x_i direction (m/s^2), C_D is the drag coefficient, R_e is relative Reynolds number, and $R_e = \frac{\rho d_p |u_{pi} - u_i|}{\mu}$.

Computational Mesh

The software ANSYS R15.0 is used to simulate the airflow field in the separation chamber. First, the software SOLIDWORKS (2013 edition) is used to establish the 2D and 3D models of separation chamber. The 2D model is taken along the longitudinal direction of separation chamber and passes through the center plane of the single-row airflow-holes. The 3D model is also along its longitudinal direction, but the area intercepted should contain several rows of same-speed airflow-holes. Whether it is for 2D or 3D model, the interception position should be far away from the wall influence area. Then, the 2D and 3D models are respectively imported into ICEM CFD R15.0 for mesh division. Unstructured grid is adopted, and gird is densely meshed at the airflow-holes of airflow component and the reticulated cylinders of suction cleaner, while the remaining part is loosely meshed. Finally, the FLENT R15.0 is used to calculate the velocity of airflow field and the movement trajectory of seed cotton within the model.

Boundary Conditions and Other Related Parameters Setting

The seed cotton moves in the separation chamber, and there are gas-solid two phases in the cavity. The gas phase is air, which is processed as incompressible and whose pressure is standard atmospheric pressure. The airflow-holes are the velocity-inlet; the reticulated cylinders are the pressure-outlet; the boundaries of reticulated cylinders are 'trap'; the boundary of cotton-outlet is 'escape', the walls are set as 'wall', and the others are in default conditions. In addition, the discrete phase is the seed cotton. According to the experience, the diameter of seed cotton is 0.03 m, the shape coefficient is 0.70 and the density is 43kg/m^3.The seed cotton adopts an entry mode of uniform surface, and its direction of entry is vertical to the cotton-inlet.

RESULTS AND DISCUSSION

Setting of Geometric and Kinematic Parameters of Model

According to the requirements of production line, if the width of equipment for removing the residual films is 1.00 m, the seed cotton processing capacity should be 4000 kg/h. To better connect with the production line, the separation chamber width B is set at 1.00 m, the length L is 2.02 m, and the cotton yield is 4000 kg/h. After many simulation experiments, certain relevant empirical data were obtained, which are as follows:

Parameters related to the cotton-inlet:$B_1 = 0.20$m, $H_1 = 0.20$ m,$\gamma = 45.00°$; parameters related to the cotton-outlet: $B_2 = 0.39$ m, $H_2 = 0.05$ m, $\theta = 45.00°$; and parameters related to the reticulated cylinders: $L_1 = 0.65$m, $L_2 = 0.75$m,R = 0.15m; parameters related to the hole-plate:$S = 0.06 - 0.08$m,$\emptyset d = 0.02$m,$S_1 = 0.03$ m, $S_2 = 0.05$ m. In addition, the velocity of seed cotton at the cotton-inlet $V_1 = 0.00$ m/s.

2D Airflow Field Characteristics and Key Parameter Optimization

In separating the residual films from the seed cotton by the air-floating, quite some factors affect the characteristics of airflow field. In addition to the above mentioned parameters, there are another four key parameters, namely, the airflow velocity at the inlet of airflow-hole, the height of separation chamber, the dip angle of walls of cotton-inlet and cotton-outlet, and the dip angle of hole-plate (or the dip angle of airflow-holes). These parameters not only individually affect the airflow field characteristics within the cavity, but also, by different combinations or different values in one combination, cause differences in flow field characteristics. To acquire the optimal combination of influencing factors as well as the combination of optimal values, the authors adopt the orthogonal experiment design. First of all, we determine experiment indexes. In order to separate the residual films from the seed cotton, the latter should be discharged from the cotton-outlet after passing the separation chamber. Besides, in order for all the residual films to be absorbed by the reticulated cylinders, the seed cotton should run in the chamber for reasonably long time. Hence, the discharging ratio of cotton exiting the separation chamber and the running time of it within the cavity should be taken as the experiment indexes, which should respectively be 100% and 5.00-6.00s according to the need. Next is about determining the experiment factors and levels selected. After lots of simulation experiments, the above-mentioned four key parameters severely affect the airflow velocity inside the separation chamber, that is, they affect the movement trajectory and running time of seed cotton. Therefore, the four parameters are used as experiment factors. To guarantee the reliability of experimental results, three levels are selected for each of the four factors. The orthogonal experiment program that combines four factors - each having three levels - is adopted, as shown

Table 1. Factor and Level

Factors	Levels		
	1	2	3
Airflow velocity at inlet of airflow-hole V (m/s)	3.80	3.85	3.90
Height of separation chamber H (m)	1.00	1.20	1.40
Dip angle of walls of cotton-inlet and cotton-outlet α (°)	90.00	85.00	80.00
Dip angle of airflow-hole β (°)	2.00	5.00	8.00

Table 2. Orthogonal Experiment Program

Program number	Factors				Results	
	V	H	α	β	Discharging ratio of seed cotton (%)	Running time (s)
1	1 (3.80)	1 (1.00)	1 (90.00)	1 (2.00)	0.00	19.81
2	1	2 (1.20)	2 (85.00)	2 (5.00)	100.00	8.24
3	1	3 (1.40)	3 (80.00)	3 (8.00)	100.00	5.13
4	2 (3.85)	1	2	3	100.00	6.11
5	2	2	3	1	100.00	8.84
6	2	3	1	2	65.00	19.21
7	3 (3.90)	1	3	2	100.00	5.68
8	3	2	1	3	0.00	8.86
9	3	3	2	1	100.00	9.97

in **Table 1**. Then the orthogonal experiment programs are present, as shown by the first five columns in **Table 2**. Lastly, experiments are conducted according to the nine combinations in **Table 2**, to obtain the airflow field characteristics and analyze the experiment results.

During experiments by the 2D model, the cross-section with the coordinate value Y=0.475m and parallel to the coordinate plane XOZ is selected as the objective, in which the airflow velocity, the discharging ratio of seed cotton and its running time in the cavity are obtained. Columns 6 and 7 of **Table 2** give the discharging ratio and running time in the cavity of seed cotton, respectively. The experiment results of the above nine combinations are classified into three categories according to the airflow field characteristics in the cross-section, and the representative ones are extracted from the three categories, as shown in **Fig. 4**. According to the airflow field characteristic of velocity (**Fig. 4 (b)**, **(d)**, **(f)** and **(h)**), the airflow field in the separation chamber can be divided into three areas: the bottom, the middle and the upper areas. The bottom area is diffusion zone of the airflow from airflow-holes on the hole-plate, where the airflow velocity is high, unstable and attenuate quickly, and the airflow field is mainly influenced by the airflow velocities at airflow-holes and its dip angle. The area is located within height of approximately 0.15m from the bottom of separation chamber. In the middle area, the airflow field is more stable, and the velocity of airflow is obviously lower than that in the bottom area. The airflow direction is mainly affected by the dip angles of walls of cotton-inlet and cotton-outlet. The area falls in the range between 0.15m and 0.5m above the bottom. Under the influence of negative-pressure reticulated cylinders, the airflows in the upper area – in the part 0.5m high and above - have relatively high velocity. In light of the airflow field characteristics of three areas, the seed cotton should run in the middle area of airflow field. In order to ensure the separation of residual films from the seed cotton, the airflow velocity in the middle area should be in the range of 1.20-3.00m/s. The three categories of airflow field characteristics are analyzed in detail below.

In **Fig. 4 (a)** and **(b)**, the airflow velocity in the middle area of airflow field is between 2.56m/s and 2.84 m/s, which meets the requirement for the residual films to rise. In the model with such airflow field, the walls of cotton-inlet and cotton-outlet are perpendicular to the horizontal plane, so the airflow velocity is small in the horizontal direction in the cavity, and the seed cotton moves to a certain distance and then falls to the hole-plate, which cannot be discharged from the cotton-outlet. In **Fig. 4 (c)** and **(d)**, the airflow velocity in the middle area is between 2.50m/s and 2.80 m/s. The residual films can rise and the seed cottons can suspend. For the model, the walls of cotton-inlet and cotton-outlet and the airflow-holes on the hole-plate are inclined to the cotton-outlet, so the airflow velocity in the horizontal direction is sufficiently high, thereby making the seed cottons move forward and get completely discharged from the cotton-outlet. In **Fig. 4 (e)**, **(f)**, **(g)** and **(h)**, the air velocity in the middle area is between 2.58 m/s and 3.19 m/s. However, the walls of cotton-inlet and cotton-outlet are vertical to the horizontal plane, the airflow velocity is small in the horizontal direction, and the seed cottons run slower. On the other hand, the airflow velocity reaches or exceeds 2.88 m/s in a large area near the cotton-outlet, and its upward velocity component is large, so part or all of the seed cottons are adsorbed by the negative-pressure reticulated cylinders and thus cannot be completely discharged from the cotton-outlet. In order to obtain the best experiment results, the influence of four factors on the discharging ratio of seed cotton and its running time in the cavity is further analyzed.

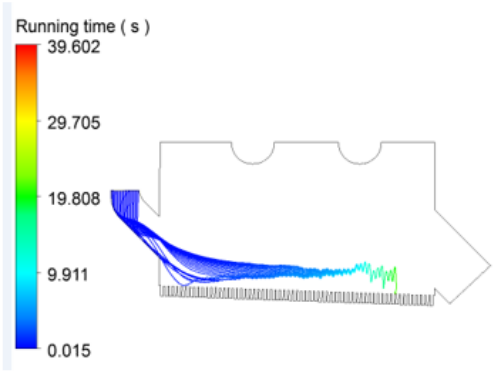

(a) Movement trajectory of seed cotton in program 1

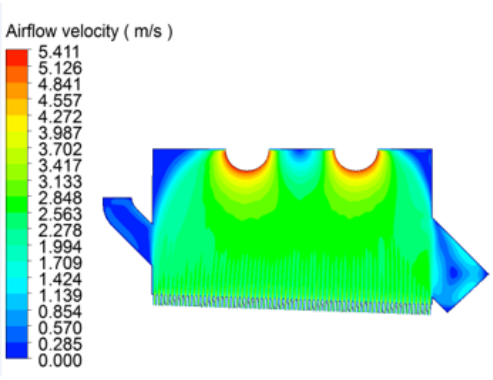

(b) Airflow velocity cloud map in program 1

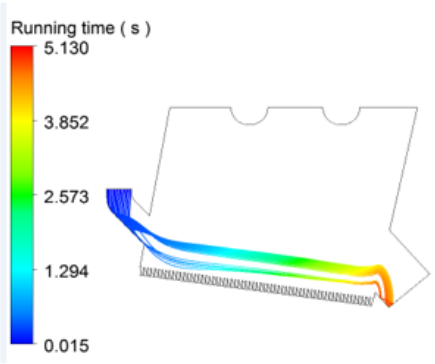

(c) Movement trajectory of seed cotton in program 3

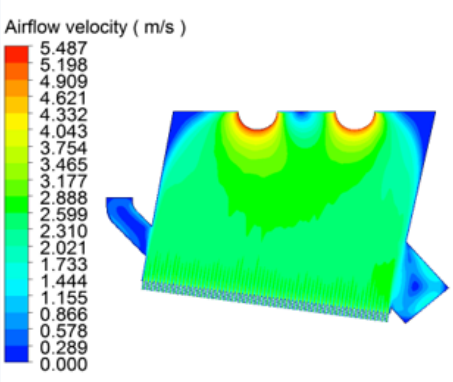

(d) Airflow velocity cloud map in program 3

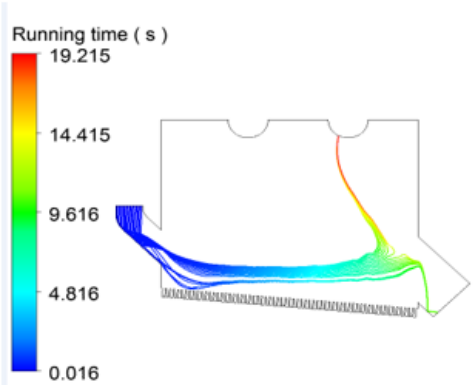

(e) Movement trajectory of seed cotton in program 6

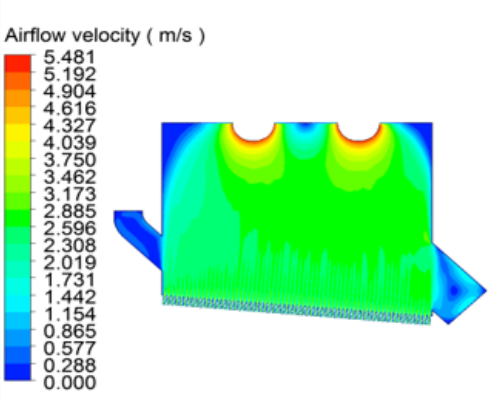

(f) Airflow velocity cloud map in program 6

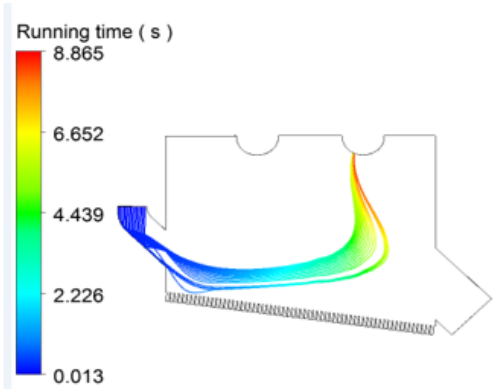

(g) Movement trajectory of seed cotton in program 8

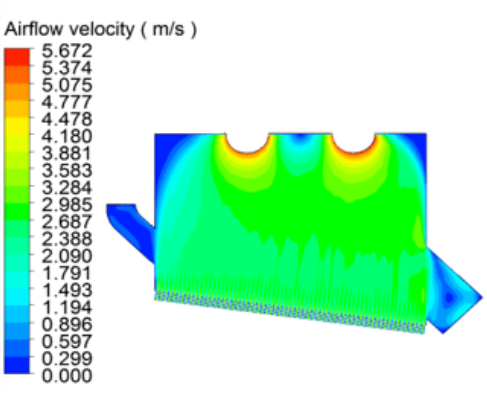

(h) Airflow velocity cloud map in program 8

Fig. 4. Movement Trajectory of Seed Cotton and Velocity Cloud Map of Airflow Field

Table 3. Analysis of Orthogonal Experiment

Experiment indexes	Calculated valuesin process	Factors			
		V	H	α	β
Discharging ratio of seed cotton	K_{1j}	200.00	200.00	65.00	200.00
	K_{2j}	265.00	200.00	300.00	265.00
	K_{3j}	200.00	265.00	300.00	200.00
	$\overline{K_{1j}}$	66.67	66.67	21.67	66.67
	$\overline{K_{2j}}$	88.33	66.67	100.00	88.33
	$\overline{K_{3j}}$	66.67	88.33	100.00	66.67
	δ_j	21.66	21.66	78.33	21.66
	Order	$\alpha > V = \mathrm{H} = \beta$			
	Optimal Combination	$V_2\mathrm{H}_3\alpha_2\beta_2$or $V_2\mathrm{H}_3\alpha_3\beta_2$			
Running time	K_{1j}	33.17	31.59	47.86	38.61
	K_{2j}	34.15	25.94	24.32	33.12
	K_{3j}	24.51	34.30	19.65	20.10
	$\overline{K_{1j}}$	11.06	10.53	15.95	12.87
	K_{2j}	11.38	8.65	8.11	11.04
	$\overline{K_{3j}}$	8.17	11.43	6.55	6.70
	δ_j	3.21	2.78	9.40	6.17
	Order	$\alpha > \beta > V >$ H			
	Optimal Combination	$V_3\mathrm{H}_2\alpha_3\beta_3$			

First, we calculate the sum of the results of the experiment indexes corresponding to each level under each factor $K_{ij}(i = 1,2,3; j = 1,2,3,4)$and the corresponding average value $\overline{K_{ij}}(i = 1,2,3; j = 1,2,3,4)$, as shown in **Table 3**. Secondly, we calculate the extreme difference corresponding to the three levels under each factor $\delta_j(j = 1,2,3,4)$; then we rank, in the order of priority, the four factors according to the range difference $\delta_j(j = 1,2,3,4)$. Next, we determine the optimal combination of individual experiment index according to the value $\overline{K_{ij}}(i = 1,2,3; j = 1,2,3,4)$ under each factor. Finally, the optimal value combination is determined by the comprehensive balance method. For the factor V, it ranks second in terms of impact on the discharging ratio, and third in terms of impact on the running time; it can take the value V_2. For the factor H, it ranks second in terms of impact on the discharging ratio, and forth in terms of impact on the running time; it can take the value H_3. For the factor α, it ranks first in terms of both impact on the discharging ratio and impact on the running time; it can take the value α_3. For the factor β, it ranks second in both the impact on the cotton discharging ratio and the impact on the running time; hence either β_2 or β_3 can be taken. But when β_3 is taken, the cotton discharging ratio is 24.52% lower than that of β_2, and the running time is reduced by 39.31%, so β_3 is taken as the value of β.

The optimal combination of values for the experiment should be $V_2\mathrm{H}_3\alpha_3\beta_3$. In **Table 2**, the third combination is $V_1\mathrm{H}_3\alpha_3\beta_3$. For the two combinations, the geometric parameters are the same, but the value of kinematic parameteris different. For the above 2D model, the airflow field is considered only in the plane, and the obtained kinematic parameter value has relatively large difference. The 2D model is only used to obtain the geometric parameter values, so the combination of optimal values of geometric parameters is $\mathrm{H}_3\alpha_3\beta_3$, that is, the height of separation chamber is 1.40m, the dip angle of walls of cotton-inlet and cotton-outletis 80.00°, and the dip angle of airflow-holes is 8.00°. To more closely reflect the characteristics of airflow field inside the separation chamber and accurately obtain the kinematic parameter value, the 3D model should be analyzed.

Analysis of 3D Airflow Field and Determination of Kinematic Parameter Value

The separation chamber was intercepted by two planes having coordinate values Y=0.40m and Y=0.50 m and parallel to the coordinate plane XOZ, respectively, and the region between the two sections is taken as a research object. Since the 'wave-pattern' airflow velocity is to be realized in the transverse direction of separation chamber (the Y axis direction), it is necessary to study the airflow velocity at each of the airflow-hole rows in the transverse direction of hole-plate. According to the geometric parameters of hole-plate in 4.1, two rows of airflow-holes should be included in the research region.

In order to better observe the airflow field in the separation chamber, the plane I is intercepted through the center line of single-row airflow-holes (i.e., the plane parallel to the coordinate plane XOZ and intersecting the Y axis at 0.475m), and the plane II is intercepted at the center position between the two rows of airflow-holes (i.e., the plane parallel to the coordinate plane XOZ plane and intersecting the Y axis at 0.450 m). It is assumed that the airflow velocities of airflow-holes are 7.00 m/s, 9.00 m/s, 12.00 m/s and 14.00 m/s, respectively.

Fig. 5 shows the velocity clouds on planes I and II when the airflow velocity of the airflow-holes is 12.00 m/s. It can be seen that the airflow is sprayed outward

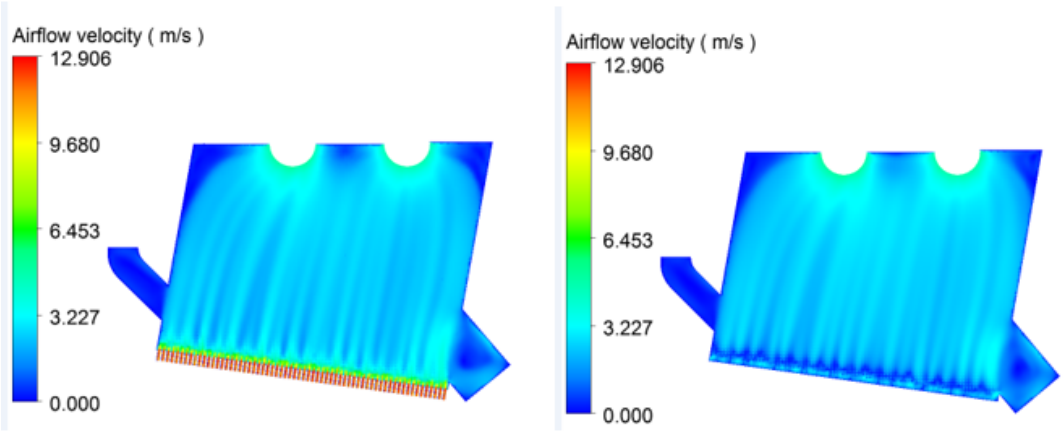

(a) Velocity cloud on plane I (b) Velocity cloud on plane II

Fig. 5. Velocity Distribution in Separation Chamber

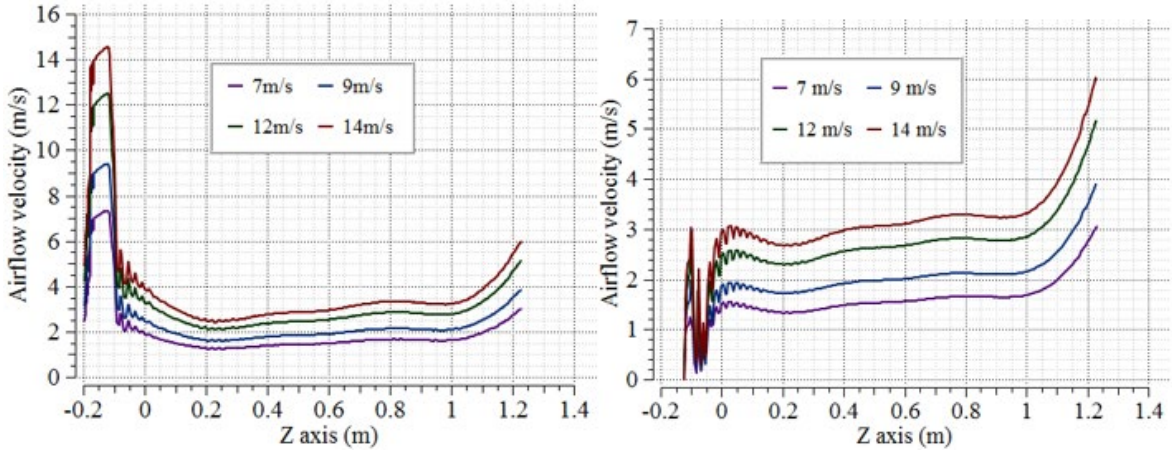

(a) Airflow velocity at intersection line Q1 (b) Airflow velocity at intersection line Q2

Fig. 6. Velocity Curve of Airflow in Separation Chamber

through the airflow-holes to form a jet, which diffuses outward from the orifices and intersects into a plane after a certain distance. The plane is about 0.10 m from the bottom of separation chamber. Therefore, the distance between the bottom of cotton-inlet and the one of separation chamber should be larger than 0.10m (0.20 m in this study), so as to ensure the smooth running of seed cotton in the separation chamber. The same result can be obtained by setting the airflow velocity at the airflow-holes at 7.00 m/s, 9.00 m/s and 14.00 m/s.

In order to study the quantitative relationship between the airflow velocity at the inlet of airflow-hole on the hole-plate and the airflow velocity in the separation chamber, the plane with the coordinate value X=0.895m and parallel to the coordinate plane YOZ (i.e., the plane is close to the center of the first reticulated cylinder) is used to cut out the research region, which intersects the above Planes I and II perpendicularly, and the intersection lines are Q1 and Q2, respectively. When the airflow velocity at the inlets of airflow-holes is 7.00 m/s, 9.00 m/s, 12.00 m/s and 14.00 m/s, respectively, the airflow velocities at the intersection lines Q1 and Q2 are as shown in **Fig. 6(a)** and **(b)**, respectively. The minimum airflow velocities corresponding to the separation chamber are 1.18 m/s, 1.70 m/s, 2.15 m/s, and 2.70 m/s, respectively. In order to maintain the airflow velocity in the middle area of airflow field between 1.20m/s and 3.00m/s, the airflow velocity at the inlets of airflow-holes should be between 8.00 m/s and 14.00 m/s, which can blow away the residual films from the seed cotton. If the airflow velocity at the inlets of airflow-holes exceeds 14.00 m/s, the seed cotton moves upward due to the airflow impacts and fails to be discharged from the cotton-outlet. In summary, if the 'wave-pattern' airflow velocity is achieved, the airflow velocity at the inlet of each row of airflow-hole on the hole-plate should be in the range of 8.00-14.00 m/s.

CONCLUSIONS

(1) The novel model is created to separate the residual film from the seed cotton, and it is the first time to propose that the seed cotton is tore into the movable 'wave-pattern' thin layer by blowing air so that the residual film is fully exposed and then cleared by the suction-cleaner. To acquire such a seed cotton layer, upward airflows that flow in the 'wave-pattern' are added to the separation chamber transversely in the model, and airflows that can carry the seed cotton forward are added to the chamber longitudinally. By adjusting the difference between the airflow velocity at the wave crest and wave trough, the thickness of seed cotton layer is set.

(2) The discharging ratio of cotton exiting the separation chamber and the running time of it within the cavity are taken as the experiment indexes, and the airflow velocity at the inlet of airflow-hole, the height of separation chamber, the dip angle of walls of cotton-inlet and cotton-outlet, and the dip angle of airflow-holes are used as experiment factors, which are used to analyze the characteristics of airflow field inside the separation chamber in the 2D model. According to its characteristics, the bottom area is diffusion zone of the airflow from airflow-holes, where the airflow velocity is high, unstable and attenuate quickly, and the airflow field is mainly influenced by the airflow velocities at airflow-holes and its dip angle. The area is located within height of approximately 0.15m from the bottom of separation chamber. The airflow field in the middle area is more stable and the airflow velocity is obviously lower than that in the bottom area, and the airflow direction is mainly affected by the dip angles of walls of cotton-inlet and cotton-outlet. The area falls in the range between 0.15m and 0.5m above the bottom. The airflow in the upper area has relatively high velocity due to the suction-cleaner. Therefore, the seed cotton should run in the middle area of airflow field. By further analyzing the orthogonal experiment results, the optimized values of three key geometric parameters are gained, that is, the height of separation chamber is 1.40m, the dip angle of walls of cotton-inlet and cotton-outlet is 80.00°, and that of airflow-holes on the hole-plate is 8.00°.

(3) In order to acquire the velocities of 'wave-pattern' airflow, the characteristics of the separation chamber's airflow field are analyzed in the 3D flow field by setting the airflow velocity at the inlet of each row of airflow-hole on the hole-plate. The results show that in order for the airflow velocity to stay in the range of 1.20-3.00m/s in the middle area of airflow field, the range of airflow velocity at the inlet of each row of airflow-hole on the hole-plate should be 8.00-14.00 m/s.

ACKNOWLEDGEMENT

This work was supported by the Agricultural Financial Project (05162130111242005).

REFERENCES

Cintron MS, Rodgers JE (2017) Identification of common cotton contaminants using an FTIR microscope with a focal plane array detector. AATCC Journal of Research, 4(6): 12-17.

Du Y, Luo Y, Jiang X, Cai W, Geng D (2016) Research of foreign fibers in cotton yarn defect model based on regression analysis. Journal of the Textile Institute, 107(9): 1089-1095.

Du Y, Ma T, Yang C, Jiang X (2017) Detection clustering analysis algorithm and system parameters study of the near-point multi-class foreign fiber. Journal of the Textile Institute, 108(6): 1022-1027.

Guo W, Kan Z, Zhang R, Guo S, An H, Cong T (2011) Analysis of material character based on mesh roller-type cotton and film remnant separator. Transactions of the CSAE, 27(Supp.2): 1-5.

Guo Y-Y, Wang X-J, Zhai Y-S, Wang C-D, Wang L-W, Zhai F-X, Yan K, Liu J, Yang H-J, Du Y-X, Zhang Z-F (2014) A novel method for identification of cotton contaminants based on machine vision. Optik, 125(6):1707-1710.

Jiang Y, Li C (2015a) Detection and discrimination of cotton foreign matter using push-broom based hyperspectral imaging: system design and capability. Plos One, 10(3): e0121969.

Jiang Y, Li C (2015b) MRMR-based feature selection for classification of cotton foreign matter using hyperspectral imaging. Computers and Electronics in Agriculture, 119: 191-200.

Kuzy J, Li C (2017) A Pulsed Thermographic Imaging System for Detection and Identification of Cotton Foreign Matter. Sensors, 17: 518.

Li Q, Han S, Wang P, Wang L, Xia W (2015) Foreign fiber detecting system based on multispectral technique.2015 International Conference on Optical Instruments and Technology: Optical Systems and Modern Optoelectronic Instruments, OIT 2015. SPIE: 96180W.

Liu X, He X, Su Z, Liu F, Wang D, Gu Q (2014) Laser imaging method for fast detecting white foreign fibers in cotton. Transactions of the Chinese Society of Agricultural Engineering (Transactions of the CSA E), 30(15): 190-196.

Mustafic A, Li C (2015) Classification of cotton foreign matter using color features extracted from fluorescent images. Textile Research Journal, 85(12): 1209-1220.

Mustafic A, Li C, Haidekker M (2014) Blue and UV LED-induced fluorescence in cotton foreign matter. Journal of Biological Engineering, 8: 29.

Peng B, Huang S, Li D (2015) Detection of colorless plastic contaminants hidden in cotton layer using chromatic polarization imaging. Chinese Optics Letters, 13(9): 092901.

Wang D, Yin B, Liu X, He X, Su Z (2015a) Laser line scan imaging method for detection of white foreign fibers in cotton. Transactions of the Chinese Society of Agricultural Engineering (Transactions of the CSAE), 31(9): 310-314.

Wang J, Du Y, Jiang X, Luo Y, Li X (2014) Classification processing method of cotton foreign fibers based on probability statistics and BP neural network. 4th International Conference on Mechanics, Simulation and Control, ICMSC 2014. Switzerland: Trans Tech Publications, p.428-431.

Wang L, Lin T, Yan C, Wang J, Guo R, Yue L, Tang Q (2016) Effects of plastic film residue on evapotranspiration and soil evaporation in cotton field of Xinjiang. Transactions of the Chinese Society of Agricultural Engineering (Transactions of the CSA E), 32(14): 120-128.

Wang X, Li D, Yang W, Li Z (2015b) Lint Cotton Pseudo-foreign Fiber Detection Based on Visible Spectrum Computer Vision. Transactions of the Chinese Society for Agricultural Machinery, 46(8): 7-14.

Wang X, Yang W, Li Z (2015c) A fast image segmentation algorithm for detection of pseudo-foreign fibers in lint cotton. Computers and Electrical Engineering, 46: 500-510.

Wei P, Zhang L, Liu X, Wang D, Su Z (2017) Detecting method of foreign fibers in seed cotton using double illumination imaging. Journal of Textile Research, 38(4): 32-38.

Yuan Z, Zhu L, Geng F, Peng Z (2013) Gas solid two phase flow and numerical simulation, Nanjing, China: Southeast University Press.

Zhang C, Sun S, Shi W, Zeng L, Deng D (2017a) Design and test of foreign fiber removal machine based on embedded system. Transactions of the Chinese Society for Agricultural Machinery, 48(8): 43-52.

Zhang H, Li D (2014) Applications of computer vision techniques to cotton foreign matter inspection: A review. Computers and Electronics in Agriculture, 109: 59-70.

Zhang L, Wei P, Wu J, Liu X, Su Z (2016) Detection method of foreign fibers in cotton based on illumination of line-laser and LED. Transactions of the Chinese Society of Agricultural Engineering (Transactions of the CSAE), 32 (15): 289-293.

Zhang M, Li C, Yang F (2017b) Classification of foreign matter embedded inside cotton lint using short wave infrared (SWIR) hyperspectral transmittance imaging. Computers and Electronics in Agriculture, 139: 75–90.

Zhao X, Li D, Yang B, Liu S, Pan Z, Chen H (2016a) An efficient and effective automatic recognition system for online recognition of foreign fibers in cotton. IEEE Access, 4: 8465-8475.

Zhao X, Li D, Yang B, Ma C, Zhu Y, Chen H (2014) Feature selection based on improved ant colony optimization for online detection of foreign fiber in cotton. Applied Soft Computing Journal, 24: 585-596.

Zhao X, Liu X, Li D, Chen H, Liu S, Yang X, Zhan S, Zhao W (2016b) Comparative study on metaheuristic-based feature selection for cotton foreign fibers recognition. Computer and Computing Technologies in Agriculture IX - 9th IFIP WG 5.14 International Conference, CCTA 2015. United States: Springer New York, p. 8-18.

Zhou W, Xv S, Liu C, Zhang J (2016) Applications of near infrared spectroscopy in cotton impurity and fiber quality detection: A review. Applied Spectroscopy Reviews, 51(4): 298-312.